Indirect-exchange interactions in zero-gap semiconductors

G. Bastard
Groupe de Physique des Solides de l'Ecole Normale Supérieure, 24 rue Lhomond, 75231 Paris Cedex 05, France

C. Lewiner
Groupe de Physique des Solides de l'Ecole Normale Supérieure, Université Paris VII, Tour 23, 2 place Jussieu, 75221 Paris Cedex 05, France
(Received 16 October 1978; revised manuscript received 27 March 1979)

The indirect-exchange interaction between two localized magnetic moments is calculated in zero-gap semiconductors. The virtual interband transitions between the valence and conduction bands give rise to an indirect-exchange mechanism which is ferromagnetic if the band degeneracy is accidental. If, however, the band degeneracy is symmetry induced, the indirect interaction is antiferromagnetic. A discussion of the magnetic susceptibility of zero-gap $Hg_{1-x}Mn_xTe$ alloys is given.

I. INTRODUCTION

In metals or degenerate semiconductors, two localized magnetic moments interact predominantly through the polarization of the electron gas. That mechanism, the RKKY (Ruderman-Kittel-Kasuya-Yosida) interaction,[1] is significant only for large numbers of carriers and leads to an interaction which oscillates as a function of the distance between the localized moments. In insulators such a mechanism is inefficient and the localized moments interact either directly, if they are close enough, or through the superexchange mechanism[2] which leads to antiferromagnetism. The zero-gap semiconductors, being the border between metals and insulators, are of interest to investigate in detail which is the indirect-exchange interaction produced by virtual electron transitions from the (filled) valence band to the almost empty conduction band. At this point, we already want to stress the crucial part which will be played by the symmetry of the band-edge Bloch functions.

Besides, there exists a whole class of "semimagnetic" zero-gap semiconductors: the $Hg_{1-x}Mn_xTe$ alloys. Magnetic-susceptibility measurements[3,4] performed on these ternary random alloys revealed that even for low Mn content, the Mn^{2+} ion magnetization departs considerably from the noninteracting spin behavior. At high temperature, a Curie-Weiss law was found, $\chi^{-1} \approx T + \Theta$, displaying an antiferromagnetic interaction between localized moments, which proved impossible to interpret by accounting only for isolated or nearest-neighbor paired Mn^{2+} moments.

Low-temperature oscillatory interband magnetoabsorption,[5] as well as magnetotransport phenomena,[6] lead to similar results. Antiferromagnetic interaction between localized spins was also evidenced, which was not possible to relate to single, pair, or triplet Mn^{2+} ions. All the previous interpretations postulated the impossibility of long-range interactions between spins. Then, only direct exchange between closely spaced moments was presented as a possible explanation of the observed phenomena.

The purpose of the present paper is to investigate the problem of indirect-exchange interaction in zero-gap semiconductors, and to compare two physical situations of interest: accidental band degeneracy or symmetry-induced degenerate band edges. Despite the small free-carrier concentrations (electrons and holes), we will show that there nevertheless exists a strong interaction, which is long range, between localized spins. This interaction originates from the virtual transitions across the zero gap between the valence and conduction bands. A similar mechanism has already been investigated by Bloembergen and Rowland[7] in open-gap semiconductors. These authors, considering two bands separated by a finite energy gap, have shown that the effective indirect-exchange interaction was exponentially decreasing with the interspin distance. Their calculations are not applicable to the present situation, which is characterized by a symmetry-induced zero-gap structure for HgMnTe alloys.

The paper will be organized as follows: in Sec. II, we compare the wave functions and effective Hamiltonians in the two situations of interest, accidental or symmetry-induced band degeneracy. We also recall the low-temperature electrical properties of zero-gap Hg chalcogenides. In Sec. III, we calculate the effective interaction between the localized moments. Section IV will be devoted to a comparison between the Curie temperature calculated from our model, and the experimental results of Savage *et al.*[3] and Andrianov *et al.*[4]

II. BAND STRUCTURES, ELECTRON WAVE FUNCTIONS, AND LOW-TEMPERATURE ELECTRICAL PROPERTIES

There exists a whole class of semiconducting materials for which the thermal gap is exactly zero. These zero-gap semiconductors may be divided into two groups.

A. Accidental band degeneracy

In the first group, the band degeneracy is accidental and may occur at an arbitrary point in the Brillouin zone. Among other substances, $Bi_{1-x}Sb_x$ alloys display such phenomena (although the zero gap is indirect). For such materials there exist *a priori* no symmetry relations between the valence and conduction bands. Any perturbation, even displaying the lattice symmetry, destroys the zero-gap structure. In the following, we will deliberately assume that both valence and conduction bands are of the simplest type (for instance, we will neglect any spin-orbit interaction and assume that the band extrema occur at the center of the Brillouin zone). These drastic approximations, already widely used for open-gap semiconductors,[7] will help to analyze the various contributions to the indirect-exchange mechanisms and to compare their orders of magnitude.

If the conduction and valence bands are fortuitously degenerate at the center of the Brillouin zone, they may be considered as being uncoupled for any value of the electron wave vector, provided k is small enough. The wave functions for electrons in both bands are

$$\psi_{c,v,\sigma}(\vec{r}) = u_{c,v,0,\sigma}\frac{\exp i\vec{k}\cdot\vec{r}}{\sqrt{\Omega}} \tag{1}$$

corresponding to the dispersion relations

$$\epsilon_c(\vec{k}) = \frac{\hbar^2k^2}{2m_c};\quad \epsilon_v(\vec{k}) = -\frac{\hbar^2k^2}{2m_v}\,. \tag{2}$$

$u_{c,v,0}$ are the periodic parts of the Bloch functions at $k=0$ and Ω is the volume of the crystal.

B. Symmetry-induced zero-gap semiconductors

1. Band structure

The symmetry-induced zero-gap semiconductors are, besides α-Sn, the cubic Hg chalogenides HgTe, HgSe, β-HgS, and some of the ternary random alloys $Hg_{1-x}Cd_xTe$, $Hg_{1-x}Mn_xTe$, etc. They have an inverted band structure as compared to InSb-like materials (Fig. 1). The two Γ_8 bands (p symmetry, $J=\frac{3}{2}$) tied up by symmetry at $k=0$ form the conduction and the valence bands, whereas a Γ_7 doublet (p symmetry, $J=\frac{1}{2}$), a split-off valence band, lies below the Γ_8 edges at an energy distance $\Delta=\epsilon_{\Gamma_8}-\epsilon_{\Gamma_7}$. Between the Γ_8 and Γ_7 bands, the Γ_6 band (s symmetry) intercalates. The thermal gap is exactly zero and the lowest-lying optical gap equals $|\epsilon_0|$ where $\epsilon_0=\epsilon_{\Gamma_6}-\epsilon_{\Gamma_8}$. In $Hg_{1-x}Mn_xTe$ alloys $|\epsilon_0|$ depends on the composition x. At $T=4.2$ K, $|\epsilon_0|$ decreases with increasing x from 0.3 eV ($x=0$) down to 0 ($x\approx 7.5\%$) where a zero-gap–semiconductor transition takes place (Fig. 1); whereas Δ remains constant $\Delta\approx 1$ eV.

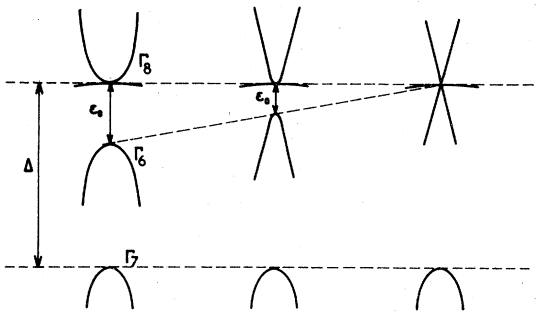

FIG. 1. Band structure of symmetry-induced zero-gap semiconductors (e.g., HgMnTe alloys).

The Γ_8 valence mass depends on remote bands, and is almost insensitive to a change in ϵ_0. The conduction mass is always very light ($m_c\approx 3\times10^{-2}m_0$ in HgTe), and decreases proportionally to $|\epsilon_0|$ for small $|\epsilon_0|$. Despite nonparabolicity phenomena, which may be quite important in the conduction band of zero-gap alloys with small $|\epsilon_0|$, we will restrict our purpose to parabolic dispersion relations and use the Luttinger[8] approach to calculate the eigenfunctions of valence and conduction levels. Such a procedure will enable us to get an exact estimate of the p symmetry of the band-edge Bloch functions, and of the effect of spin-orbit coupling. This parabolic approximation will be valid for $Hg_{1-x}Mn_xTe$ alloys of $x\lesssim 1\%$.

Neglecting the warping, the Luttinger effective Hamiltonian reads

$$\mathcal{H}_0(\vec{k}) = \frac{1}{8}\left(\frac{9}{2}\frac{\hbar^2}{m_c}+\frac{1}{2}\frac{\hbar^2}{m_v}\right)k^2 - \frac{1}{2}\left(\frac{\hbar^2}{2m_v}+\frac{\hbar^2}{2m_c}\right)(\vec{k}\cdot\vec{J})^2\,. \tag{3}$$

It is of interest to note that the $\vec{k}\parallel\vec{z}$ conduction ($M_J=\pm\frac{1}{2}$) and valence ($M_J=\pm\frac{3}{2}$) eigenstates are no longer eigenstates for arbitrary $\vec{k}$. The diagonalization of $\mathcal{H}_0(\vec{k})$ depends on the direction of $\vec{k}$,[8,9] whereas in the case of accidental band degeneracy, the effective Hamiltonian is diagonal, whatever the direction of the electron wave vector.

When projected on the basis $|\frac{3}{2},\frac{3}{2}\rangle$; $|\frac{3}{2},-\frac{1}{2}\rangle$; $|\frac{3}{2},\frac{1}{2}\rangle$, $|\frac{3}{2},-\frac{3}{2}\rangle$, the eigenstates corresponding to positive eigenvalues $\epsilon_c(k)=\hbar^2k^2/2m_c$ read $[\vec{k}=(k,\theta,\phi)]$

$$\psi_{e^+}=\frac{\exp i\vec{k}\cdot\vec{r}}{\sqrt{\Omega}}\begin{pmatrix}-\frac{1}{2}\sqrt{3}\sin\theta\, e^{-i\phi}\\ \frac{1}{2}\sin\theta\, e^{i\phi}\\ \cos\theta\\ 0\end{pmatrix},$$

$$\psi_{e^-}=\frac{\exp i\vec{k}\cdot\vec{r}}{\sqrt{\Omega}}\begin{pmatrix}0\\ \cos\theta\, e^{-i\phi}\\ -\frac{1}{2}\sin\theta\, e^{-2i\phi}\\ -\frac{1}{2}\sqrt{3}\sin\theta\end{pmatrix}, \tag{4}$$

whereas the wave functions of valence-band electrons corresponding to $\epsilon_v(k)=-\hbar^2k^2/2m_v$ are

$$\psi_{h^+}=\frac{\exp i\vec{k}\cdot\vec{r}}{\sqrt{\Omega}}\begin{pmatrix}\cos\theta\, e^{-3i\phi}\\ 0\\ \frac{1}{2}\sqrt{3}\sin\theta\, e^{-2i\phi}\\ \frac{1}{2}\sin\theta\end{pmatrix},$$

$$\psi_{h^-}=\frac{\exp i\vec{k}\cdot\vec{r}}{\sqrt{\Omega}}\begin{pmatrix}-\frac{1}{2}\sin\theta\, e^{-3i\phi}\\ -\frac{1}{2}\sqrt{3}\sin\theta\, e^{-i\phi}\\ 0\\ \cos\theta\end{pmatrix}. \tag{5}$$

In other words, the wave functions of conduction and valence electrons can still be expressed as

$$\psi_{n\vec{k}\sigma}=u_{n\vec{k}\sigma}\frac{\exp i\vec{k}\cdot\vec{r}}{\sqrt{\Omega}}, \tag{6}$$

but the periodic parts of the Bloch functions now depend explicitly on $\vec{k}$. Note also that $\pm$ subscripts in Eqs. (4) and (5) take care of the Kramers degeneracy of both bands. They should be confused neither with the bare-electron spin σ_z nor with J_z, the z component of the total angular momentum. Again these complications arise from the Γ_8 symmetry of the band edge.

2. *Free-electron and free-hole concentrations at low temperatures*

As before we restrict our analysis to parabolic zero-gap $Hg_{1-x}Mn_xTe$ alloys ($x\lesssim 1\%$). For these materials only the low-temperature properties are of relevance, the temperature range 0–30 K being enough to observe the Curie-Weiss behavior. At these low temperatures the free-electron and -hole concentrations are dominated by impurity effects. They are quite peculiar in zero-gap materials[10,11]: the acceptor levels fall in the continuum of the conduction band, whereas the donor levels occur in the valence-band background. Therefore, strictly speaking, bound acceptor (or donor) states do not exist. However, owing to the marked difference between the valence and conduction masses ($m_c/m_v \ll 1$), it has been established[10,11] that acceptor impurities may give rise to quasidiscrete resonant acceptor levels, whereas the donor resonances are always overdamped and the donor levels ionized at any temperature. As a consequence, even if the number of acceptors N_A exceeds the number of donors N_D, the materials behave at low temperatures as n-type semiconductors: the electrons are free whereas the holes are trapped on the acceptor levels. For the A_1 acceptor level, corresponding to Hg vacancies, $\epsilon_{A_1}\approx 2.2$ meV and with $N_D/\Omega\sim 2\times10^{15}$ cm^{-3}, $N_A/\Omega\approx 10^{16}$ cm^{-3} the concentration of free electrons is $n\sim N_D/\Omega \approx 2\times10^{15}$ cm^{-3}. As for the Fermi level, it is close to the acceptor level for $T\lesssim 10$ K (Fig. 2). For higher temperatures, typically $10\lesssim T\lesssim 30$ K, two mechanisms compete[10]: thermal activation of electron-hole pairs and thermal hopping of electrons on the unoccupied acceptor levels. A minimum appears in the curve $n(T)$, whereas the number of free holes is nonvanishing. Let us however note that the holes remain statistically nondegenerate, whereas the electron gas is degenerate. Besides the holes have also a much lower mobility ($\mu_p\sim 5\times10^2$ cm^2 V s) than the electrons ($\mu_n\sim 10^5-10^6$ cm^2 V s).

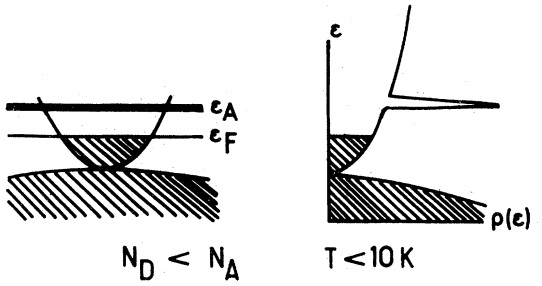

FIG. 2. Density of states [$\rho(\epsilon)$] and band filling of symmetry-induced zero-gap semiconductors with $N_D < N_A$, $T < 10$ K.

III. INDIRECT-EXCHANGE HAMILTONIAN

The mobile (in Γ_8 bands) and localized d electrons (which form the magnetic moments) are assumed[5,6] to interact via the Heisenberg-type Hamiltonian

$$\mathcal{H}_{\rm int}=\sum_{\vec{R}_i}J(\vec{r}-\vec{R}_i)\,\vec{S}_i\cdot\vec{\sigma}\,, \tag{7}$$

where $\vec{S}_i$ are localized spins located at $\vec{R}_i$ and $\vec{\sigma}$ the bare-electron spin. $J(\vec{r}-\vec{R}_i)$ is an exchange integral centered at $\vec{R}_i$ and varying rapidly over a unit cell.

The first-order energy shift produced by $\mathcal{H}_{\rm int}$ van-

ishes, since it is proportional to the localized spin magnetization, which we assume to be zero (paramagnetic state).

The second-order energy shift reads

$$\Delta\epsilon^{(2)} = \sum_{\substack{i,f \\ \vec{k},\vec{k}'}} \frac{f(\epsilon_{ik})[1-f(\epsilon_{fk'})]}{\epsilon_{ik}-\epsilon_{fk'}} |\langle i\,\vec{k}\,|\mathcal{H}_{\rm int}|f\,\vec{k}'\rangle|^2 , \quad (8)$$

which, owing to the rotational invariance of the unperturbed Hamiltonian, may be rewritten in the form of the effective spin-spin Hamiltonian. By restricting ourselves to isotropic terms we get

$$\Delta\epsilon^{(2)} = \sum_{i>j} I(\vec{R}_{ij})\,\vec{S}_i\cdot\vec{S}_j . \quad (9)$$

$I(\vec{R}_{ij})$ may be decomposed into interband and intra-conduction-band and intra-valence-band contributions.

$$I_{ij}^{\rm inter} = \frac{2}{\Omega^2}\sum_{\vec{k},\vec{k}'} \frac{f(\epsilon_{vk'})[1-f(\epsilon_{ck})]}{\epsilon_{vk'}-\epsilon_{ck}} \exp[i(\vec{k}-\vec{k}')\cdot\vec{R}_{ij}] \times \sum_{\sigma,\sigma'=\pm} |\langle u_{c\vec{k}\sigma}|J(r)\sigma_z|u_{v\vec{k}'\sigma'}\rangle|^2 , \quad (10)$$

where the isotropic assumption has been again used to express all the required matrix elements in terms of those involving σ_z. Similarly the intra-conduction-band term becomes

$$I_{ij}^{\rm intra} = \frac{1}{\Omega^2}\sum_{\vec{k},\vec{k}'} \frac{f(\epsilon_{ck})-f(\epsilon_{ck'})}{\epsilon_{ck}-\epsilon_{ck'}} \exp[i(\vec{k}-\vec{k}')\,\vec{R}_{ij}] \times \sum_{\sigma,\sigma'=\pm} |\langle u_{ck\sigma}|J(r)\sigma_z|u_{ck'\sigma'}\rangle|^2 . \quad (11)$$

The intra-valence-band contribution is given by a similar expression.

The main problem is now to evaluate the matrix elements appearing in Eqs. (10) and (11). Hence the symmetries of the band-edge Bloch functions play a crucial part. In the case of fortuitous degeneracy, these matrix elements are independent of the electron wave vector $\vec{k}$ and $\vec{k}'$ because the $u_{ak\sigma}(r)$ are themselves independent of $\vec{k}$. For symmetry-induced band degeneracy this is not the case, and the required matrix elements will depend on $\vec{k}/k$ and $\vec{k}'/k'$. Such an angular variation will not affect the R_{ij} dependence of $I_{ij}^{\rm inter}(k_F=0)$ (k_F is the Fermi wave vector), which is actually imposed by the double summation over $\vec{k}$ and $\vec{k}'$ in Eq. (10). It will however sensitively alter the strength of this interaction, leading even to a change of its sign, as will be seen below.

We will now analyze more precisely both cases of accidental or symmetry-induced band degeneracy.

A. Accidental band degeneracy

We will assume: (i) that the bare electron spin $\vec{\sigma}$ is a good quantum number; (ii) that the Fermi level in the conduction band is finite [$\epsilon_F = (\hbar^2 k_F^2/2m_c)$]. The intra-conduction-band contribution then reduces to the usual RKKY formula

$$I_{ij}^{{\rm intra},c} = \frac{\alpha_c^2 m_c k_F^4}{32\pi^3\hbar^2}\left|\frac{-\sin 2y + 2y\cos 2y}{y^4}\right| , \quad (12)$$

where

$$\alpha_c = \langle u_{c0}|J(r)|u_{c0}\rangle , \quad R = R_{ij} , \quad y = k_F R .$$

The intra-valence-band term is discussed in Appendix A; we recall here only its expression

$$I_{ij}^{{\rm intra},v} = \frac{-\alpha_v^2 m_v}{16\pi^{5/2}\hbar^2 R^4}\left(\frac{2m_v R^2 k_B T}{\hbar^2}\right)^{3/2}\exp(-\beta\epsilon_F) \times \exp\left(-\frac{2m_v R^2 k_B T}{\hbar^2}\right) . \quad (13)$$

We may cast the interband term into the form

$$I_{ij}^{\rm inter} = I_{ij}(k_F=0) + \delta I_{ij}(k_F\neq 0) , \quad (14)$$

which exhibits the contribution for $k_F=0$ and the correction δI_{ij} due to a finite Fermi level.

The former contribution reads

$$I_{ij}^{\rm inter}(k_F=0) = -\frac{m_v\alpha_{cv}^2}{2\pi^3\hbar^2 R^4}\frac{s}{(1+s^2)^2} , \quad (15)$$

with $\alpha_{cv} = \langle u_{c0}|J(r)|u_{v0}\rangle$ and $s = (m_v/m_c)^{1/2}$. Its sign arises directly from the negative value of the denominator in Eq. (10) and thus gives a ferromagnetic contribution.

Contrarily to the case of open-gap semiconductors,[7] we obtain a power-law variation of $I_{ij}(k_F=0)$ with the distance R: $I_{ij}^{\rm inter}(k_F=0)\approx R^{-n}$, $n=4$. This power law is imposed by the zero-gap structure and will be the same for the case of symmetry-induced band degeneracy. As may be seen in Eq. (10), the value of the exponent ($n=4$) is a direct consequence of the parabolic dispersion law and of the dimensionality.

$I_{ij}^{\rm inter}(k_F=0)$ vanishes when $s\to\infty$, but keeps a constant sign. It decreases in both limits $s\to 0$, $s\to\infty$, i.e., when the bands are strongly asymmetric. This behavior is due to the decreasing part played by the $k\approx 0$ range of the spectrum: it is in the case of nearly symmetrical bands that the virtual transitions, occurring at vanishing or small energies, extend over the largest k range providing $I^{\rm inter}(k_F=0)$ with its maximum value. As for $\delta I_{ij}^{\rm inter}(k_F\neq 0)$, it is given by

$$\delta I_{ij}^{\rm inter}(k_F\neq 0) = \frac{m_v\alpha_{cv}^2}{2\pi^3\hbar^2 R^4}\left[\frac{s}{(1+s^2)^2} - \frac{1}{2}e^{-sy}\left(\frac{y}{1+s^2}(\cos y + s\sin y) + \frac{1}{(1+s^2)^2}[(s^2-1)\sin y + 2s\cos y]\right)\right] . \quad (16)$$

In the presence of a finite Fermi energy, the interband contribution $I_{ij}^{\text{inter}}(k_F=0)+\delta I_{ij}^{\text{inter}}(k_F\neq 0)$ shows its R^{-4} dependence multiplied by exponentially decreasing and oscillating functions. The exponential decrease is due to the presence of the Moss-Burstein gap between the uncoupled valence and conduction levels, whereas the oscillations are due to the finite k_F. These oscillations would be absent if a true gap existed between both bands (virtual creation of electron-hole pairs at $\vec{k}=0$).

In order to compare the intraband and interband contributions, we have inserted the total exchange integral into a molecular-field-type approximation (see Appendix B). This calculation shows that the interband term provides a much larger contribution to the Curie-Weiss temperature than the intraband terms (if $\alpha_{cv}\approx\alpha_c\approx\alpha_v$) for usual electron concentrations ($10^{14}<n<10^{17}$ cm^{-3}). Of course if the electron concentration becomes very large, the RKKY interaction prevails over interband terms: the zero-gap anomaly becomes irrelevant, and the material behaves like a metal.

B. Symmetry-induced band degeneracy

In the actual case of symmetry-induced band degeneracy, some of the above conclusions will still be valid, for instance the intraband terms will remain negligible with respect to the interband contribution. Nevertheless we will discuss in detail the intra-conduction-band contribution since (a) heavily doped n-type zero-gap materials can be easily prepared (e.g., $Hg_{1-x}Mn_xSe$ alloys or doped $Hg_{1-x}Mn_xTe$ alloys[6]); (b) there is an academic interest in examining the modifications of RKKY formula due to Γ_8 wave functions.

To calculate I_{ij}^{inter} and $I_{ij}^{\text{intra,}c}$ we have to evaluate the matrix elements of $J(\vec{r})\sigma_z$ between the $k\neq 0$ and $k'\neq 0$ valence and conduction Bloch functions accounting for the Kramers degeneracy of each band. The presence of a large spin-orbit coupling leads to nonvanishing matrix elements between states of different pseudospin. Denoting by β the matrix $\langle X|J(\vec{r})|X\rangle$, replacing σ_z by $\frac{1}{3}J_z$ (valid in the Γ_8 multiplet), and expressing wave vectors in spherical coordinates, one obtains

$$\sum_{\sigma,\sigma'=\pm}|\langle c\,\vec{k}\,\sigma|J(\vec{r})\sigma_z|c\,\vec{k}\,'\sigma'\rangle|^2=\left(\frac{\beta}{12}\right)^2(-39\cos^2\theta-39\cos^2\theta'+45\cos^2\theta\cos^2\theta'+41)$$
$$+\left(\frac{3\beta}{12}\right)^2[\cos(\phi-\phi')\sin2\theta\sin2\theta'-\sin^2\theta\sin^2\theta'\cos2(\phi-\phi')]\ , \tag{17}$$

$$\sum_{\sigma,\sigma'=\pm}|\langle c\,\vec{k}\,\sigma|J(\vec{r})\sigma_z|v\,\vec{k}\,'\sigma'\rangle|^2=\beta^2[-\tfrac{5}{16}\cos^2\theta\cos^2\theta'+\tfrac{5}{48}-\tfrac{1}{16}\cos^2\theta+\tfrac{13}{48}\cos^2\theta'$$
$$-\tfrac{1}{16}\sin2\theta\sin2\theta'\cos(\phi-\phi')+\tfrac{1}{4}\sin^2\theta\sin^2\theta'\cos2(\phi-\phi')]\ . \tag{18}$$

Owing to the cylindrical symmetry around the R_{ij} axis, the terms involving $\phi-\phi'$ do not contribute to the effective interaction I_{ij}. The intra-conduction-band term is symmetrical with respect to the interchange of θ and θ', whereas the interband term does not show such behavior owing to the asymmetry between valence and conduction wave functions. Both interband and intraband contributions are the sum of a spherically symmetric term, which will give rise to effects exactly similar to the ones previously calculated [Eqs. (12)–(16)], and to angular dependent terms which will lead to new and important features. After straightforward (and tedious) calculations it becomes

$$I_{ij}^{\text{inter}}(k_F=0)=-\frac{\beta^2 m_c m_v}{4\pi^4\hbar^2R^4}\int_0^\infty x^2\,dx\int_0^\pi\sin\theta\,d\theta\,e^{-ix\cos\theta}\int_0^\infty\frac{t^2\,dt}{m_ct^2+m_vx^2}$$
$$\times\int_0^\pi\sin\theta'\,d\theta'e^{it\cos\theta'}(-\tfrac{5}{16}\cos^2\theta\cos^2\theta'+\tfrac{5}{48}-\tfrac{1}{16}\cos^2\theta+\tfrac{13}{48}\cos^2\theta')\ , \tag{19}$$

$$I_{ij}^{\text{inter}}(k_F=0)=-\frac{\beta^2 m_v}{16\pi^3\hbar^2R^4}f(s)\ , \tag{20}$$

where

$$f(s)=-\frac{s}{1+s^2}+\tfrac{1}{2}\pi-\arctan s+\frac{13}{3s}\frac{1}{1+s^2}-3s^2\arctan s\ ; \tag{21}$$

$$\delta I_{ij}^{\text{inter}}(k_F \neq 0) = \frac{\beta^2 m_v}{16\pi^3\hbar^2 R^4}\left[\left(\frac{6s}{(1+s^2)^2}+\frac{13}{3s}\frac{1}{1+s^2}\right)[1-e^{-sy}(\cos y + s\sin y)] - \frac{3e^{-sy}}{1+s^2}(y\cos y - \sin y + 2y\sin y)\right.$$
$$-\frac{13}{3s^2}[\text{si}(y) - E\,\text{si}(y)] + (y\cos y - \sin y)\left(3e^{-sy}+\frac{5}{sy}e^{-sy}-\frac{5}{s^2y^2}(1-e^{-sy})\right)$$
$$-\sin y\, e^{-sy}(1-3sy) + E\,\text{si}(y) - \frac{7s}{1+s^2}+\frac{6s^3}{(1+s^2)^2}+\frac{3s^2}{1+s^2}\sin y\, e^{-sy}$$
$$\left.+e^{-sy}(\cos y + s\sin y)\left(\frac{7s}{1+s^2}-\frac{6s^3}{(1+s^2)^2}-\frac{3s^2 y}{1+s^2}\right)\right]; \tag{22}$$

$$I_{ij}^{\text{intra},c} = \frac{m_c}{8\pi^3\hbar^2 R^4}\frac{\beta^2}{36}\left[78[\text{si}(y)-\text{si}(2y)] - 7\sin 2y + 2y\cos 2y + \frac{90}{y}(\cos y - \cos 2y) + \frac{45}{y^2}(\sin 2y - 2\sin y)\right], \tag{23}$$

with

$$y = k_F R, \quad s = \left(\frac{m_v}{m_c}\right)^{1/2}, \quad \text{si}(x) = \int_0^x \frac{\sin t\, dt}{t}, \quad E\,\text{si}(x) = \int_0^x \frac{\sin t}{t} e^{-ts}\, dt\ .$$

Let us first examine the k_F-dependent contributions [Eqs. (22) and (23)]. Their behaviors are compared in Tables I and II to the results obtained in the case of accidental band degeneracy for both limits $k_F R \to 0$ and $k_F R \to \infty$. $I_{ij}^{\text{intra},c}$ behaves asymptotically like the usual RKKY interaction, but the numerical factors when $k_F R \to 0$ or $k_F R \to \infty$ do not coincide, due to the angular dependence of the electron wave functions. A sketch of $I_{ij}^{\text{intra},c}$ is presented in Fig. 3, together with the RKKY curve.

As for $\delta I_{ij}^{\text{inter}}(k_F \neq 0)$ contributions, they are in both cases antiferromagnetic near the origin and always prevail over the intraband term ($m_v/m_c \gg 1$). However, the behaviors of $I_{ij}^{\text{inter}}(k_F = 0) + \delta I_{ij}^{\text{inter}}(k_F \neq 0)$ at large $k_F R$ sharply contrast in the two cases of interest. For accidental band degeneracy one finds an exponential decrease, whereas for symmetry-induced band degeneracy a power-law decline is obtained: $I_{ij}^{\text{inter}} \approx R^{-5}\cos k_F R$. Its origin may be traced back to the interband matrix elements of $J(R)\sigma_z$ which are not spherically invariant. On Fig. 4, we show the variations of I_{ij}^{inter} vs y, obtained in the two cases mentioned above.

Actually, owing to the very small k_F value existing in zero-gap materials, the limit $k_F R \approx \infty$ is of no great practical significance. For instance, at $T = 4.2$ K in $Hg_{1-x}Mn_xTe$ alloys with $x < 1\%$, $m_c \approx 3\times 10^{-2} \times m_0$, $m_v \approx 0.4 m_0$, $\epsilon_F \approx 2$ meV one gets $k_F R \approx 1$ for $R \approx 200$ Å, i.e., of the order of the mean free path of valence electrons. As shown by de Gennes,[12] for interspin distances much larger than the mean free path l_0 it is meaningless to use unperturbed (by impurities) electron states in the second-order energy shift: qualitatively all the interactions become

TABLE I. Comparison between the $k_F R$ dependences of $I_{ij}^{\text{intra},c}$ for accidental and symmetry-induced band degeneracies. $y = k_F R$.

$I_{ij}^{\text{intra},c}$	Accidental degeneracy (RKKY)	Symmetry-induced degeneracy
$\lim_{k_F R \to 0} I_{ij}^{\text{intra},c}$	$-\frac{m_c}{4\pi\hbar^2}\frac{\alpha_c^2}{R}n$	$-\frac{7}{72}\frac{m_c}{\pi\hbar^2}\frac{\beta^2}{R}n$
$\lim_{k_F R \to \infty} I_{ij}^{\text{intra},c}$	$\frac{m_c\alpha_c^2}{16\pi^3\hbar^2 R^4}y\cos 2y$	$\frac{m_c\beta^2}{144\pi^3\hbar^2 R^4}y\cos 2y$

TABLE II. Comparison between the $k_F R$ dependences of $\delta I_{ij}^{\text{inter}}(k_F \neq 0)$ for accidental and symmetry-induced band degeneracies. $y = k_F R$, $\tan\eta = s^{-1}$.

$\delta I_{ij}^{\text{inter}}(k_F \neq 0)$	Accidental degeneracy	Symmetry-induced degeneracy
$\lim_{k_F R \to 0} \delta I_{ij}^{\text{inter}}(k_F \neq 0)$	$\dfrac{m_v \alpha_{cv}^2}{4\pi\hbar^2 R} n$	$\dfrac{\beta^2 m_v}{24\pi\hbar^2 R} n$
$\lim_{k_F R \to \infty} \delta I_{ij}^{\text{inter}}(k_F \neq 0)$	$-I_{ij}^{\text{inter}}(k_F=0)\left[1 - \dfrac{1}{2}\dfrac{(1+s^2)^{3/2}}{2} y e^{-sy} \sin(y+\eta)\right]$	$-I_{ij}^{\text{inter}}(k_F=0)\left[1 + \dfrac{58}{3s^2 f(s)} \dfrac{\cos y}{y}\right]$

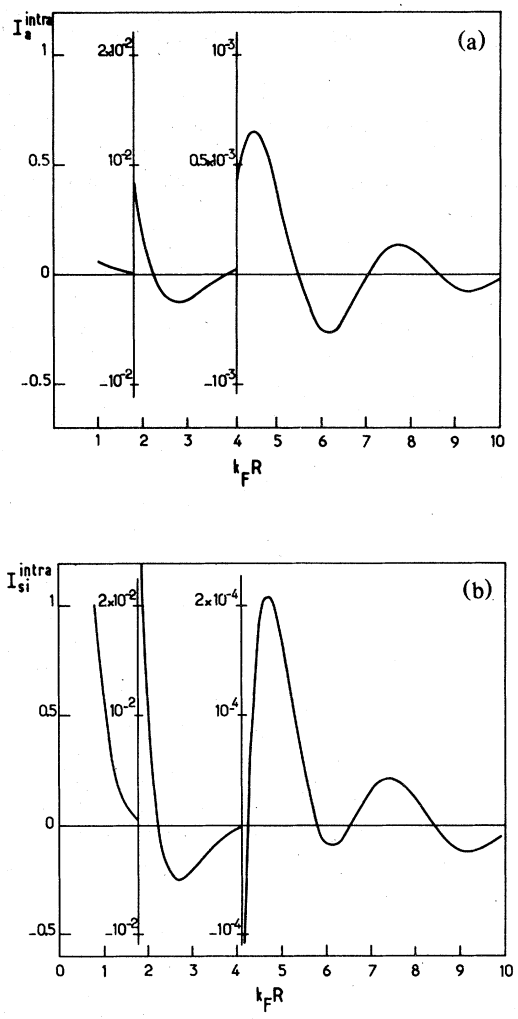

FIG. 3. Intraband contributions to I_{ij} for $s=4$. (a) Plot of $-(16\pi^3\hbar^2/\alpha_c^2 k_F^4 m_v) I_{ij}^{\text{intra},c}$ vs $k_F R$ in the case of accidental degeneracy. (b) Plot of $-(16\pi^3\hbar^2/\beta^2 k_F^4 m_v) I_{ij}^{\text{intra},c}$ vs $k_F R$ in the case of symmetry-induced degeneracy.

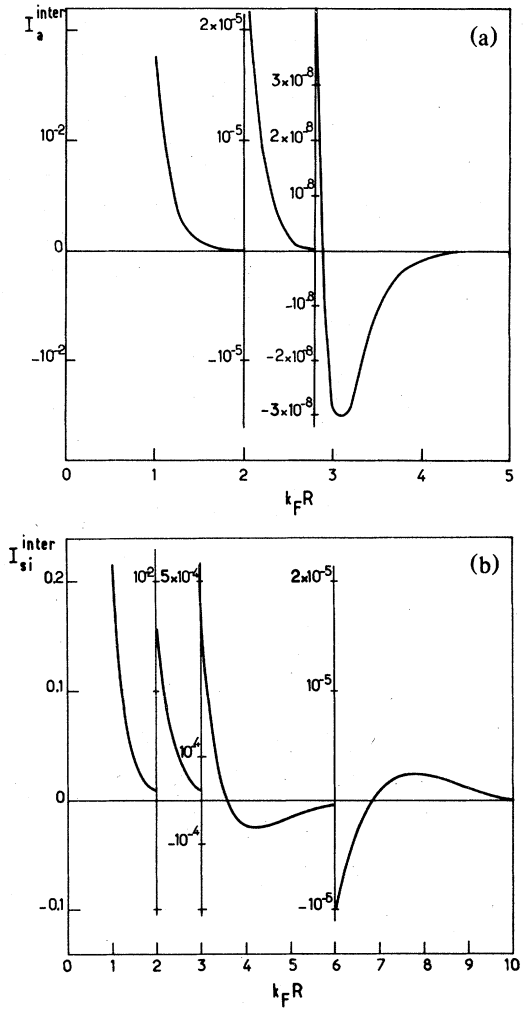

FIG. 4. Interband contributions to I_{ij} for $s=4$. (a) Plot of $-(16\pi^3\hbar^2/\alpha_{cv}^2 k_F^4 m_v)[I_{ij}^{\text{inter}}(k_F=0) + \delta I_{ij}^{\text{inter}}]$ vs $k_F R$ in the case of accidental degeneracy. (b) Plot of $(16\pi^3\hbar^2/\beta^2 k_F^4 m_v)[I_{ij}^{\text{inter}}(k_F=0) + \delta I_{ij}^{\text{inter}}]$ vs $k_F R$ in the case of symmetry-induced degeneracy.

screened by an exponential term $\exp(-R/l_0)$. In any case, at low temperature (say $T < 40$ K) for $Hg_{1-x}Mn_xTe$ alloys with $x < 1\%$, the k_F-dependent terms may be safely approximated by their limit $k_F R \to 0$ owing to the very low values of Fermi energy ($\epsilon_F < 20$ meV).

These limiting values have to be compared with $I_{ij}^{\text{inter}}(k_F = 0)$: from Table II and Eq. (20), it is obvious that these terms are negligible compared to $I_{ij}^{\text{inter}}(k_F = 0)$ for all reasonable distances. We may thus conclude that at low temperature, for zero-gap materials which are not intentionally n-type doped, *the dominant indirect-exchange term is* $I_{ij}^{\text{inter}}(k_F = 0)$ *characterized by the* R^{-4} *power-law variation.*

We will now examine further Eq. (20), the main feature being its dependence upon s. The variation of $f(s)$ upon s is shown on Fig. 5. Contrary to zero-gap materials with accidental band degeneracy, the symmetry-induced zero-gap semiconductors display, in the limit of infinite spin-orbit coupling, an indirect-exchange mechanism whose *sign* depends on the ratio between valence and conduction masses. $f(s)$ shows a sign reversal near $s \approx 0.5$. However, for all existing materials $s > 3$: the indirect-exchange mechanism due to the virtual interband transitions is then *antiferromagnetic.*

This sign reversal again arises from the angular dependence of the interband matrix elements. At large s, the dominant term in $f(s)$ is $-(13\pi/6)s^{-2}$, a contribution which originates from the $\cos^2\theta'$ term appearing in Eq. (19). The latter leads, after integration over θ', to the second derivative of $(\sin t)/t$. The integral over t shows two poles: one on the imaginary axis which leads to exponentially decreasing terms in x, and the other at $t = 0$ which arises from the term in t^{-3}. Such a pole leads to a power-law decline in x [see Eq. (19)], which in turn gives rise to the $-(13\pi/6)s^{-2}$ term.

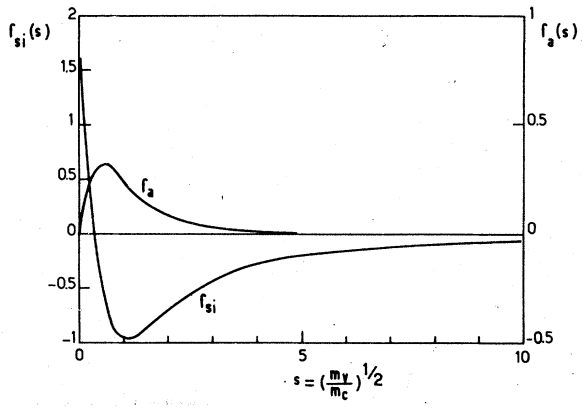

FIG. 5. Dependence of the effective exchange integral at $k_F = 0$ upon s in the cases of accidental degeneracy (f_a) and of symmetry-induced degeneracy (f_{si}).

To conclude this discussion, we have attempted to separate the relative influence of our two assumptions: (a) symmetry-induced band degeneracy, (b) infinite spin-orbit coupling. Hence we have examined in Appendix C the case of a symmetry-induced zero-gap semiconductor with $\Delta = 0$. It just so happens that $I_{ij}^{\text{inter}}(k_F = 0)$ is always positive if $\Delta = 0$. We may then conclude that in the case of existing zero-gap materials ($s > 1$), the antiferromagnetic exchange interaction entirely originates from the symmetry-induced band degeneracy. In fact, the two Γ_8 bands behave like two halves of the same band, and for instance the interband-term behavior ($R^{-5}\cos k_F R$) recalls the intraband one [$R^{-3}\cos 2k_F R$ (Ref. 13)] (see Tables I and II).

IV. DISCUSSION: THE MAGNETIC SUSCEPTIBILITY OF ZERO-GAP $Hg_{1-x}Mn_xTe$ ALLOYS

The indirect-exchange mechanism due to virtual interband transitions is not weak: for a material with band parameters similar to HgTe, $R \approx 6.4$ Å (second nearest neighbor), and $N_0\beta = 1.5$ eV,[5,6] where N_0 is the number of unit cells per unit volume, one finds $I_{ij} \approx 0.2$ meV. The interband mechanism provides a natural explanation of the observed[3,4] antiferromagnetic interaction between Mn^{2+} localized moments already reported in the high-temperature susceptibility measurement. In the molecular-field approximation [high T (Ref. 14)] one finds for dilute alloys

$$\chi^{-1} = a(T + \Theta), \quad \Theta > 0 ,$$

where

$$k_B\Theta = \frac{35x}{12}\frac{\beta^2 m_v |f(s)|}{16\pi^3\hbar^2 a_0^4}\sum_{j\neq 0}\left(\frac{a_0}{R_{j0}}\right)^4 . \tag{24}$$

x is the Mn content and the summation runs over all the sites of an fcc lattice with lattice parameter a_0. If we calculate Θ for an alloy with $x = 1\%$, and assuming that the summation over lattice sites is of the order of 94, we get $\Theta \approx 6.9$ K in agreement with experiments ($\Theta_{\text{exp}} \approx 6$ K).

However, we would like to stress that the composition dependence of the Curie temperature can be quite complicated for alloys with larger x. In fact, let us transform Eq. (24) into a more convenient expression

$$k_B\Theta = -\frac{455x\beta^2\epsilon_0(x,T)m_0}{768\pi^3 E_p\hbar^2}\sum_{j\neq 0}\left(\frac{a_0}{R_{j0}}\right)^4, \quad \epsilon_0 < 0 , \tag{25}$$

where E_p is Kane's matrix element. To derive Eq. (29), we have retained the dominant term in $f(s)$ at large s and use Kane's model[15] to express m_c in terms of ϵ_0 and E_p ($m_0/m_c = -2E_p/3\epsilon_0$). We may first note that the composition dependence of Θ upon

x may not be linear, since besides the explicit linear in x variation expressing the probability that an Mn atom occupies a given site and contributes to the molecular field at the origin, there exists an implicit x dependence included in the variation of ϵ_0 with x. It is however premature to make a detailed comparison between Eq. (25) and the experimental results already reported in alloys with $x \gg 1\%$, since the band parameters ($\epsilon_0, s, \ldots$) of $Hg_{1-x}Mn_xTe$ alloys are known only for $T \approx 4$ K, whereas the determination of Curie temperature in alloys of large x requires a study of $\chi(T)$ at high temperature. At $T = 4.2$ K $\epsilon_0(x_0) = 0$ for $x_0 \approx 7$–7.5%. A comparison with $Hg_{1-x}Cd_xTe$ of similar zero-gap structures gives $\epsilon_0(x_0) = 0$ for $x \approx 4$–5% at room temperature. In any case, Θ/x may vary sensitively with x. It was also noted by Savage *et al.* that the experimental Θ could depend on the temperature scale at which $\chi(T)$ is measured. This may be related to the large temperature dependence of ϵ_0 in zero-gap materials [e.g., ϵ_0 (HgTe) varies by nearly a factor of 2 between 77 K and room temperature].

The last difficulty, which precludes a quantitative comparison between our model and the experiments, is due to the nonparabolicity effects which are entirely absent in our description. With a decrease of ϵ_0, the conduction band becomes severely nonparabolic as one easily reaches electron kinetic energies comparable or larger than $|\epsilon_0|$. One part of the indirect-exchange integral over conduction-band states is made convergent by an exponential function of the argument kRs. The parabolic approximation will then be meaningful only if the k range of interest in this integral is smaller than

$$k_0 \approx \left(\frac{2m_c|\epsilon_0|}{\hbar^2}\right)^{1/2},$$

i.e., if $R \gtrsim R_{\min}$ where

$$R_{\min} = \left(\frac{\hbar^2}{2m_v|\epsilon_0|}\right)^{1/2}.$$

For alloys with $x \lesssim 1\%$ at $T = 4.2$ K, i.e., $200 \leq |\epsilon_0| \leq 300$ meV, $R_{\min} \approx 6$ Å: the parabolic approximation is fair for almost all the interspin distances. For $Hg_{1-x}Mn_xTe$ alloys with $x \approx 4\%$ and high temperature, i.e., vanishing ϵ_0, the overall procedure becomes dubious since the summation appearing in Eqs. (24) and (25) is essentially controlled by closely separated spins (say third or fourth nearest neighbor). Another consequence of nonparabolicity phenomena is the admixture of Γ_8 with Γ_6 wave functions. This in turn decreases the proportion of p levels into conduction-band wave functions (because of normalization) and could lead to a decrease of the effective interaction between localized spins. On the other hand, the $\Gamma_6 \rightarrow \Gamma_8$ nonparabolicity induced interband contribution to the indirect-exchange mechanism may become significant. Its exponential decrease (due to the finite ϵ_0) with distance allows it to be neglected in alloys with large ϵ_0 (i.e., in "parabolic" alloys). For alloys with low ϵ_0, it should be taken into account. Clearly such effects need a detailed investigation.

The susceptibility measurements have also shown a marked departure from the Curie-Weiss behavior at low temperature: χ^{-1} curve tends to extrapolate to zero rather than to $-\Theta$. Such behavior can definitely not be interpreted by the molecular-field formulas Eqs. (19) and (24). We do not believe this invalidates our model which, in the respect of, e.g., parabolic approximation, retains its maximum relevance (the lower T, the larger $|\epsilon_0|$). A possible spin-glass formation may be credited to interpret these features, although there is no characteristic cusp in the $\chi(T)$ curves. Actually, nearest-neighbor antiferromagnetic interactions taking place on a random alloy were shown to lead to such a spin-glass phase owing to the frustration phenomena.[16]

V. CONCLUSION

The indirect-exchange interaction between localized magnetic moments has been investigated in zero-gap semiconductors. The results are summarized in Table III. The virtual interband transitions were

TABLE III. Comparison between the results obtained for zero-gap semiconductors with accidental band degeneracy (ABD) and symmetry-induced band degeneracy (SIBD). $\tan\eta = s^{-1}$.

	$k_F = 0$, $I_{ij}^{\text{inter}}(R)$	$k_F = 0$, sgn of I_{ij}	$k_F \neq 0$, $I_{ij}^{\text{intra},c}$	$k_F \neq 0$, $I_{ij} + \delta I_{ij}(R \rightarrow \infty)$
ABD	R^{-4}	ferromagnetic	RKKY	$R^{-3}\exp(-k_F R)\sin(k_F R + \eta)$
SIBD	R^{-4}	$\Delta = 0$ antiferromagnetic $\Delta = \infty$ antiferromagnetic if $s > 0.5$	complicated oscillations	$R^{-5}\cos k_F R$

shown to play a decisive part and to lead to ferromagnetic interaction between localized spins if the degeneracy is accidental, and to antiferromagnetic coupling if the zero gap is due to symmetry-induced degenerate band edges.

Whereas the power law $I^{\text{inter}} \approx R^{-4}$ originates only from the absence of energy gap between valence and conduction bands and is the result of simple dimensionality arguments, the sign of the indirect-exchange interaction is crucially dependent on the details of the band structure. Besides, for Γ_8 band edge, the symmetry coupling between valence and conduction bands leads to departure from the usual RKKY formula. Our model of indirect-exchange interaction provides a plausible explanation of the temperature dependence of the magnetic susceptibility observed in $Hg_{1-x}Mn_xTe$ zero-gap alloys with low x. A more complete interpretation is still lacking because of the unknown high-temperature band parameters of these alloys. The influence of nonparabolicity phenomena needs to be elucidated.

Note added in proof. Recent calculations[18] have shown that besides the isotropic indirect-exchange interaction $I_{ij}\vec{S}_i \cdot \vec{S}_j$, there also exists a pseudodipolar term. This term, as well as other anisotropic corrections, will be discussed in a separate publication.

ACKNOWLEDGMENTS

The authors would like to thank Professor P. Noziéres for suggesting the problem and for his illuminating comments. We are also grateful to Dr. J. Ginter, Dr. J. Kossut, and Dr. L. Swierkowski for communicating to us their results before publication.

APPENDIX A: RKKY CONTRIBUTION FOR A NONDEGENERATE HOLE GAS

In this Appendix we calculate the intravalence contribution to indirect-exchange mechanism and prove that it is negligibly small in the hole freeze-out regime. We have

$$I_{ij}^{\text{intra},v} = \frac{1}{\Omega^2} \sum_{\vec{k},\vec{k}'} \exp i(\vec{k}-\vec{k}')\vec{R}_{ij} \frac{f(\epsilon_{vk}) - f(\epsilon_{vk'})}{\epsilon_{vk} - \epsilon_{vk'}} \times \sum_{\sigma\sigma'} |\langle u_{vk\sigma}|J(r)\sigma_z|u_{vk'\sigma'}\rangle|^2 .$$

Let us for simplicity assume: a single parabolic spherical valence band: $\epsilon_{vk} = -\hbar^2k^2/2m_v$; that spin is a good quantum number; that the hole gas is nondegenerate:

$$1 - f(\epsilon_{vk}) = \exp(-\beta\epsilon_F)\exp[-\beta(\hbar^2k^2/2m_v)] ;$$

$\epsilon_F > 0$: at $T = 0$ holes are frozen onto acceptor levels. Then

$$I_{ij}^{\text{intra},v} = \frac{-\alpha_v^2 m_v}{4\pi^3\hbar^2R^4}\exp(-\beta\epsilon_F)\int_0^\infty x\sin x\cos x \times \exp\left[-\beta\frac{\hbar^2x^2}{2m_vR^2}\right]dx ,$$

with $R = R_{ij}$,

$$\alpha_v = \langle u_{v,k=0}|J|u_{v,k=0}\rangle .$$

Finally

$$I_{ij}^{\text{intra},v} = -\frac{\alpha_v^2 m_v}{16\pi^{5/2}\hbar^2R^4}\left[\frac{2m_vR^2k_BT}{\hbar^2}\right]^{3/2}\exp(-\beta\epsilon_F) \times \exp\left[-\frac{2m_vR^2k_BT}{\hbar^2}\right], \quad (26)$$

which has to be compared with the RKKY formula for a degenerate hole gas

$$I_{ij}^{\text{intra}} = -\frac{\alpha_v^2 m_v}{16\pi^3\hbar^2R^4}(-k_FR\cos 2k_FR + \tfrac{1}{2}\sin 2k_FR) . \quad (27)$$

Equation (26) shows that the lack of a sharp-hole Fermi surface kills the oscillatory behavior of I_{ij}^{intra} at large distance. Moreover the R^{-3} power-law decline at infinity [Eq. (27)] is replaced by an exponential cutoff. Finally at very low temperatures $\beta\epsilon_F \to \infty$, I_{ij} vanishes exponentially due to the absence of any free hole to interact elastically with localized moment (it is clear that the contributions of trapped holes are completely negligible at moderate doping).

APPENDIX B: COMPARISON BETWEEN Θ^{inter} AND Θ^{intra}

In order to get an insight of the order of magnitude of the different contributions to the Curie-Weiss temperature we write[14]

$$\chi^{-1} = a(T + \Theta) ,$$

where

$$k_B\Theta = \tfrac{1}{3}S(S+1)\sum_{j>i}(I_{ij}^{\text{intra},c} + I_{ij}^{\text{intra},v} + I_{ij}^{\text{inter}}) . \quad (28)$$

To obtain analytical results, we restrict our calculations to zero-gap materials with accidental band degeneracy. Furthermore we replace the discrete summation in Eq. (28) by an integration

$$\sum_{j>i}\phi(R_{ij}) \approx \frac{1}{a_0^3}\int_{R>a_0} d^3R\,\phi(R) .$$

a_0 is of the order of the lattice spacing. Then we get

from Eqs. (12), (13), and (15)

$$k_B\Theta=\frac{1}{3}\frac{S(S+1)}{a_0^3}\left[\frac{-\alpha_c^2 m_c k_F}{4\pi^2\hbar^2}\frac{\sin 2k_F a_0}{2k_F a_0}\right.$$
$$\left.-\frac{\alpha_v^2 m_v}{8\pi^{3/2}\hbar^2}\left(\frac{2m_v k_B T}{\hbar^2}\right)^{1/2}\exp(-\beta\epsilon_F)\exp\left(-\frac{2m_v a_0^2 k_B T}{\hbar^2}\right)-\frac{2m_v\alpha_{cv}^2}{\pi^2\hbar^2}\frac{s}{(1+s^2)^2 a_0}\right]. \quad (29)$$

To enable a simple comparison between intraband and interband contributions we have neglected $\delta I_{ij}^{\text{inter}}(k_F\neq 0)$ in Eq. (29). We have then

$$\frac{\Theta^{\text{inter}}}{\Theta^{\text{intra},c}}=\frac{16s^3}{(1+s^2)^2}\frac{1}{\sin 2k_F a_0}\frac{\alpha_{cv}^2}{\alpha_c^2}.$$

If $\alpha_{cv}\approx\alpha_c$ and $10^{14}<n<10^{17}$ cm^{-3} then

$$2.4\times10^1<\frac{\Theta^{\text{inter}}}{\Theta^{\text{intra},c}}<2.4\times10^2. \quad (30)$$

As for the ratio $\Theta^{\text{intra},c}/\Theta^{\text{intra},v}$ it is equal to

$$\frac{\Theta^{\text{intra},c}}{\Theta^{\text{intra},v}}=\left(\frac{\alpha_c}{\alpha_v}\right)^2\frac{2}{s^3\sqrt{\pi}}(\beta\epsilon_F)^{1/2}\exp\beta\epsilon_F. \quad (31)$$

At very low temperature say $T=4.2$ K, $\epsilon_F\approx 2.2$ meV and

$$\frac{\Theta^{\text{intra},c}}{\Theta^{\text{intra},v}}\approx 30, \quad (32)$$

whereas in the intrinsic regime $\beta\epsilon_F\approx 3$ and

$$\frac{\Theta^{\text{intra},c}}{\Theta^{\text{intra},v}}\approx 0.8. \quad (33)$$

Equations (30)–(33) clearly show that the intraband contributions are negligible with respect to the interband term. At low temperatures, in the hole-freeze-out regime the RKKY contribution [Eq. (12)] greatly prevails over the intravalence term [Eq. (13)]. As far as we are interested in low x alloys with $\Theta<7$ K, the hole contribution can be safely neglected. Moreover the very high hole damping will even increase the ratio $\Theta^{\text{intra},c}/\Theta^{\text{intra},v}$.

APPENDIX C: INDIRECT-EXCHANGE INTERACTION IN A SPIN-ORBITLESS ZERO-GAP MATERIAL

In this Appendix we calculate the interband contribution to the indirect-exchange interaction in the case of symmetry-induced zero-gap materials assumed to be spin orbitless. This will help to separate the respective influence of symmetry-induced degeneracy and infinite spin-orbit coupling on the sign of the indirect interaction. We want however to stress the fact that there exists no zero-gap semiconductor fulfilling both assumptions $\Delta=0$ and symmetry-induced degenerate band edges. Since the spin-orbit energy $\Delta=\epsilon_{\Gamma_8}-\epsilon_{\Gamma_7}$ almost entirely originates from the atomic spin-orbit coupling of the anion, it is exceedingly large in Te compounds (in HgMnTe alloys $\Delta\approx 1$ eV, $|\epsilon_0|<0.3$ eV); it is weaker in Se materials (in HgMnSe, $\Delta\approx 0.4$ eV,[17] $|\epsilon_0|<0.27$ eV); Δ could be small enough in HgS or HgO but for these materials the cubic phase is unstable compared to the hexagonal one. For instance under usual conditions HgS is a hexagonal insulating material (cynabar) and the zero-gap β-HgS can hardly be obtained. Besides HgS is always a degenerate n-type material as HgSe.

Let us however derive I_{ij}^{inter} for a symmetry-induced zero-gap material assumed to have $\Delta=0$. In that case there are two identical effective Hamiltonians corresponding to the two directions of the free spin $\vec{\sigma}$,

$$H_{\text{eff}}(\vec{k})=\left[\frac{\hbar^2k^2}{2m_c}-\frac{1}{2}\hbar^2\left(\frac{1}{m_c}+\frac{1}{m_v}\right)(\vec{k}\cdot\vec{L})^2\right]\delta_{\sigma\sigma'},$$

where $L=1$. If $\vec{k}\parallel\vec{z}$ the solution corresponding to $L_z=0$ is the electron band and those corresponding to $L_z=\pm1$ describe the two heavy hole bands. Proceeding as in the main body of the paper we get

$$\sum_{\sigma\sigma'}|\langle v\vec{k}\,\sigma|J\sigma_z|c\vec{k}\,'\sigma'\rangle|^2$$
$$=\tfrac{1}{2}\beta^2(1+\cos^2\theta+\cos^2\theta'-3\cos^2\theta\cos^2\theta')$$

and finally

$$I_{ij}^{\text{inter}}(k_F=0)=-\frac{m_v}{4\pi^3\hbar^2}\frac{\beta^2}{R^4}g(s),$$

where

$$g(s)=\frac{1}{s}-\frac{1}{2}\pi+\arctan s-\frac{1}{s^2}\arctan s.$$

As $g(s)<0$ for all s, we are led to the conclusion that the interband contribution to the indirect-exchange interaction is always antiferromagnetic.

Thus the sign of the interaction at large s (realistic case) is entirely a consequence of a symmetry-induced degenerate band edge (whereas depending on $\Delta=0$ or $\Delta=\infty$, one finds $I_{ij}\gtrless 0$ at small s).

[1]C. Kittel, Solid State Phys. 22, 1 (1968).
[2]P. W. Anderson, Solid State Phys. 14, 99 (1963).
[3]H. Savage, J. J. Rhyne, R. Holm, J. R. Cullen, C. E. Carroll, and E. P. Wohlfarth, Phys. Status Solidi B 58, 685 (1973).
[4]D. Andrianov, F. Gimel'farb, P. Kushnir, I. Lopatinskii, M. Pashkovskii, A. Savelev, and V. Fistul, Sov. Phys. Semicond. 10, 66 (1976).
[5]G. Bastard, C. Rigaux, Y. Guldner, J. Mycielski, and A. Mycielski, J. Phys. (Paris) 39, 87 (1978).
[6]M. Jaczynski, J. Kossut, and R. R. Gałazka, Phys. Status Solidi B 88, 73 (1978).
[7]N. Bloembergen and T. J. Rowland, Phys. Rev. 97, 1679 (1955).
[8]J. M. Luttinger, Phys. Rev. 102, 1030 (1955).
[9]G. L. Bir and G. E. Pikus, Sov. Phys. Solid State 3, 2221 (1962).
[10]B. L. Gelmont and M. I. Dyakonov, Sov. Phys. JETP 35, 377 (1972).
[11]L. Liu, in *Proceedings of the Third International Conference on the Physics of Narrow Gap Semiconductors* (PWN—Polish Scientific Publishers, Warsaw, 1977); G. Bastard, in *Proceedings of the Fourteenth International Conference on the Physics of Semiconductors,* edited by B. L. H. Wilson, IOP Conf. Ser. No. 43 (IPPS, London, 1979).
[12]P. G. de Gennes, J. Phys. (Paris) 23, 630 (1962).
[13]It may be remarked that the Coulombic resonant acceptor state wave function in HgTe-like zero-gap materials first decreases exponentially (with a characteristic length equal to the heavy hole Bohr radius), then shows a power-law decline and finally, when $r \rightarrow \infty$, exhibits oscillations due to the finite value of m_c (see Ref. 10). If the band degeneracy were accidental, the power-law decline would be absent.
[14]C. Kittel, *Introduction to Solid State Physics* (Wiley, New York, 1956).
[15]E. O. Kane, J. Phys. Chem. Solids 1, 249 (1957).
[16]L. de Séze, J. Phys. C 10, L353 (1977).
[17]Y. Guldner, M. Dobrowolska, C. Rigaux, A. Mycielski, and W. Dobrowolski, *Proceedings of the Third International Conference on the Physics of Narrow Gap Semiconductors* (PWN—Polish Scientific Publishers, Warsaw, 1977).
[18]J. Ginter, J. Kossut, and L. Swierkowski (private communication), and Phys. Status Solidi B (to be published).